20. Gerardin, D., Streesing, N., Cipolla Jr., J. W., and Morse, T. F., One Dimensional Unsteady Thermophoretic Motion, ibid., pp. 31-37.

21. Hayes, L. J., Devloo, P., and Spann, M. L., Finite Element Model of a Plasma Spray Coating Process, ibid., pp. 25-29.

22. Chan, C., Mazumder, J., and Chen, M. M., A two-Dimensional Transient Model for Convection in Laser Melted Pools, ibid., pp. 71-79.

23. Lin, M. L., and Eager, T. W., Influence of Surface Depression and Convection on Arc Weld Pool Geometry, idid., pp. 63-69.

24. Hou, C. A., and Tsai, C. L., Theoretical Analysis of Weld Pool Behavior in the Pulsed Current GTAW Process, ibid., pp. 117-127.

25. Weerasinghe, V. M., and Steen, W. M., Computer Simulation Model for Laser Cladding, ibid., pp. 15-23.

26. Tseng, A. A., A Numerical Heat-Transfer Analysis of Strip Rolling, ibid., pp. 55-62.

27. Prantil, V. C., and Dawson, P. R., Application of a Mixture Theory to Continuous Casting, ibid., pp. 47-54.

28. Arimond, J., and Erwin, L., Modelling of Continuous Mixers in Polymer Processing, ibid., pp. 91-98.

29. Shen, S. F., and Kwon, T. H., Boundary Integral Formulation for Creeping Flows with Application to Polymer Processing, ibid., pp. 81-89.

30. Givler, R. C., A Numerical Technique for the Prediction of Short-Fiber Orientation Resulting from the Suspension Flow, ibid., pp. 99-103.

31. Jeffrey, G. B., The Motion of Ellipsoidal Particles Immersed in a Viscous Fluid, Proceedings of Royal Society, Series A, vol. 102, pp. 161, 1923.

32. Folger, F., and Tucker III, C. L., Orientation Behavior of Fibers in Concentrated Suspensions, ASME PED-vol. 10, HTD-vol. 29, pp. 105-115, 1983.

New Developments in Two-Phase Flow Heat Transfer with Emphasis on Nuclear Safety Research

F. MAYINGER
Technical University Munich
FRG

INTRODUCTION

The literature on two-phase flow - with and without heat transfer - shows an explosive-like growth of published papers within the last ten years. Many of these papers were published as a result of nuclear safety research. It is impossible to deal with all new developments reported in this extensive literature. So one has to ask: Are there trends of special interest, where this report could be concentrated on? Looking over the situation, there seem to be three very promising fields of research having high practical actuality, especially for nuclear safety, namely:
- fluiddynamic and thermodynamic nonequilibrium in steady state,
- transient conditions,
- scaling.
The discussion on new developments in two-phase flow heat transfer, therefore, will be limited on these subjects.

FLUIDDYNAMIC AND THERMODYNAMIC NONEQUILIBRIUM

One-component vapour-liquid flow is - strictly speaking - always in a thermo- and fluiddynamic nonequilibrium condition, even if there is no heat transfer, because pressure drop on the flow path generates continuous evaporation which changes vapour content and slip ratio between the phases. Also in adiabatic two-component gas-liquid flow with no heat and mass transfer between the phases there are many situations where fluiddynamic nonequilibrium - changes of flow pattern and of the velocity ratio between the phases - exists. Usually, this disequilibrium does not affect heat transfer very much. However, there is a special situation where it can govern the heat transport from a wall. Such a condition is given with anular flow, where the liquid film cooling the wall is strongly dependent on the droplet entrainment in the vapour core. A reliable knowledge of the amount of liquid entrained in the vapour core is not only of great benefit for a better analysis of different phenomena like momentum- and heat transfer at the phase interfaces, but also is an urgent need for the design of heat exchanger components. Only by knowing the thickness of the liquid film at the wall it is possible to predict the dryout reliably.

The reason for separating droplets out of the liquid film at the wall are surface waves, as unanimously assumed in the literature.

In addition, vapour bubbles generated at the wall and penetrating the liquid film promote entrainment. Liquid droplets, however, are not only separated out of the liquid film and entrained into the vapour core, they are also replaced again - called de-entrainment - into the liquid film. Only if the amount of entrained and de-entrained droplets is equal, the fluiddynamic conditions are in equilibrium. In reality, there are three different regions along the flow path of the two-phase mixture:
- A first in which the droplet separation out of the liquid film into the vapour core prevails,
- a second in which the de-entrainment - replacing of droplets onto the liquid film - is larger, and finally,
- a third one where is equilibrium between entrainment and de-entrainment.

There is an extensive literature on entrainment measurements and predictions (see, for example, /1-5/). To calculate the entrainment one has to use a momentum balance between the droplet-enriched vapour core and the liquid anulus, which is rather difficult to formulate due to the fact that the spectrum of the droplet diameter, the velocity difference between droplet and vapour and the shear stress at the liquid film surface are not known. A simplified calculation was, for example, performed by Langner /5/ which predicts measured results quite well.
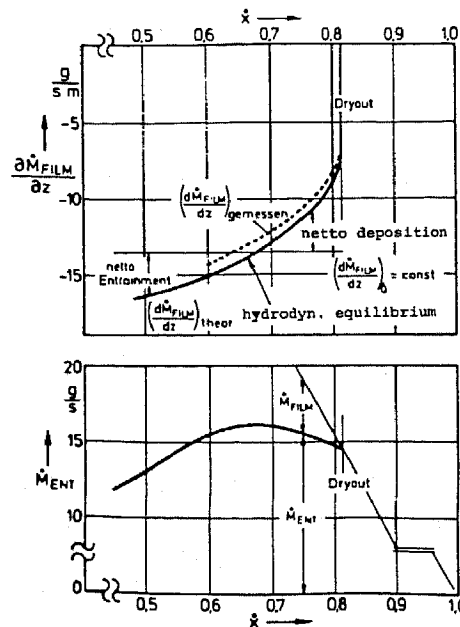

FIGURE 1. Entrainment as function of quality $\dot{x}$
(Fluid: R12, $\dot{m}$ = 500 kg/m²s,
p = 12,8 bar, Δh_{in} = 3,03 kJ/kg,
$\dot{q}$ = $\dot{q}_{Bo,5m}$ = 3,88 W/cm²;
L = 5 m, D = 0,014 m.)

In Figure 1, as an example, the liquid mass carried in the core is shown as it was measured in a tube of 5 m length and 14 mm inner diameter. Flowing substance was the refrigerant R12 at a pressure of 12,8 bar. In this figure one can distinguish two regions: one, where the droplet separation and another, where the droplet deposition prevails. In the upper diagram of Fig.1 the derivative of the film mass flow rate is shown, which is the diminution of the film, and the lower diagram gives the entrainment of droplets in the vapour core. Both diagrams are plotted versus the quality $\dot{x}$. The liquid is evaporating on its way through the tube by heat addition and, therefore, the increase of the quality $\dot{x}$ is proportional to the length of way the two-phase mixture has passed through the tube. The abscissa in Fig.1, therefore, can also be regarded as the coordinate of the flow path along the tube axis. In the upper part of Fig.1 two curves are shown; one representing the calculated values by Langner /5/ and the other, the dotted one, shows measured results. If the decrease of the liquid film would be only caused by the evaporation due to heat addition, the gradient of the liquid film thickness versus quality and also versus the tube length would be constant, because the tube had constant heat flux density. The heat flux density was, during this experiment, adjusted in a way that at the end of the 5 m long tube dryout occurred. This had the advantage that for calculating the film thickness and the entrainment a well-defined boundary condition existed.

At low quality - that is in the lower part of the tube - the decrease of the liquid film thickness is larger than it would correspond to the evaporation. This means that the separation of liquid particles prevails the deposition. This is the entrainment-governed region. At high qualities the decrease of the liquid film is smaller than it would correspond to the amount evaporated. Here, therefore, the evaporation is compensated by droplet re-deposition. Fluiddynamic equilibrium exists in this diabatic two-phase flow at this position, at which the entrainment curve is crossing the horizontal line of constant rate of evaporation (see upper diagram of Fig.1). Transfering this crossing point from the upper diagram in Fig.1 to the lower one, one realizes that this is the position where the entrainment shows a maximum. Philosophically one could say that nature tries to stabilize the situation, because a liquid film which is too thin would cause the danger of dryout, which is compensated for a while by increasing deposition. This effect can be explained with the flow pattern and the velocity distribution in the vapour core. At low quality and high entrainment the velocity profile is flat, whereas at high quality it takes the form of a parabola. The forces rectangular to the flow direction onto the droplets are larger in the latter flow situation than with a flat profile having almost constant velocity.

Thermodynamic nonequilibrium exists in two regions of a boiling channel which are far away from each other; the first one is the subcooled boiling zone at the entrance of the channel, and the second one is the post-dryout region. Subcooled boiling was frequently studied in the literature, especially for local voids in water-cooled reactors. This void is a function of the growing and the condensing of the vapour bubbles. The condensing velocity of vapour bubbles in a subcooled liquid was studied in the last years more in detail /6,7/. It was found that up to Jakob-numbers Ja = $\rho_F \cdot c \cdot \Delta T / \rho_D \cdot \Delta h_v$ = 100 the condensation of the vapour bubbles and the subcooled liquid is governed by the heat transfer at the phase interface. The temperature difference ΔT in the Jakob-number is formed with the subcooling of the liquid. The heat transfer coefficient at the phase boundary is mainly a function of the Reynolds-number, which is formed with the relative velocity between bubble and liquid, and of the Prandtl-number, as Chen /7/ showed:

$$Nu = 0,185 \, Re^{0,7} Pr^{0,5}; \tag{1}$$

The influence of the Prandtl-number, as measured by Chen /7/ with different substances, is demonstrated in Figure 2. The holographic interferograms presented there are taken at approximately identical values of Reynolds- and Jakob-numbers. The Prandtl-number influences the heat transfer at the phase interface mainly via the thickness of the boundary layer on the liquid side.
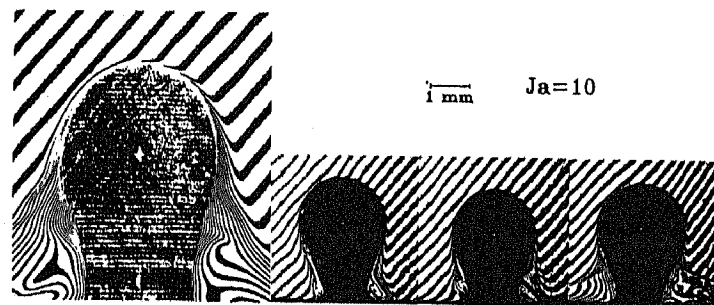

Ja=10
1 mm

FIGURE 2. Comparison of boundary layer conditions around a condensing bubble for different Pr-numbers.

	Water	R113	Ethanol	Propanol
Re=	250	300	290	320
Pr=	1.97	6.7	9.0	14.4
Nu∞=	20	41	52	63
α=	5280 [W/m²K]	1430	2930	3470

Chen /7/ presented also a correlation for the time-dependent volume of a condensing bubble with the Fourier-number $Fo = a_F \cdot t / D_{Bl,Dep}^2$ as dimensionless time.

$$D_{Bub}/D_{Bub,max} = (1 - 0.56 \ Re^{0.7} \cdot Pr^{0.5} \cdot Ja \cdot Fo)^{0.9} \qquad (2)$$

Post-dryout heat transfer is the other situation where large thermodynamic nonequilibrium exists between the phases. These heat transfer conditions exist in fossil-fired boilers of the Benson-type and during certain accident situations in the core of nuclear reactors. Older physical models predicting the heat transfer under post-dryout conditions only take in account the fluiddynamic influence of the droplets, but neglect the high thermodynamic disequilibrium between the superheated vapour and the droplets being on saturation temperature. Newer models, as - for example - presented by Iloeje /8/, Plummer /9/, Ganic /10/ or Groeneveld /11/, split the heat transport from the wall to the fluid in different parts to describe the disequilibrium between the phases. They distinguish between
- convective heat transport from the wall to the vapour,
- convective heat transport from the wall to droplets being for a moment in a non-wetting contact with the wall,
- heat transport to droplets wetting the wall,
- convective heat transport from the superheated vapour to the droplets entrained in the vapour,
- radiation from the wall to the vapour,
- radiation from the wall to the droplets.

To get good agreement between the predictions by these models and measurements, the spectrum of the droplet diameters, the variable concentration of the droplets over the flow cross section, the relative velocity between droplet and vapour and, last not least, the boundary conditions at the wall, have to be known. Schnittger /12/ checked the predictions of different models (8-11) with own measurements and found that an additional physical phenomenon is, probably, missing. He, finally, came up with the idea that the complicated

heat transfer behaviour along the flow path during post-dryout can only be explained if a droplet fragmentation is assumed. Iloeje /8/ mentioned such a fragmentation, and he explained this phenomenon with a very brief contact of the droplets on the wall without wetting it. Schnittger /12/ sees another possibility for dispersing a large droplet in a number of small particles. He assumes that the high superheating of the vapour boundary layer at the wall does not allow the droplet to contact the wall and makes large velocity differences in this boundary layer, and shear stresses resulting from it, responsible for droplet fragmentation. Based on his measurements and on the balance equations for energy and momentum he developed a new model /12/ for predicting post-dryout heat transfer. His theoretical predictions agree well with measured data in vertical upflow, as well as in horizontal flow, as Figure 3 demonstrates. In the case of horizontal flow the model gives only a mean temperature between the upper and lower part of the tube, which slightly overestimates the situation at the lower part.
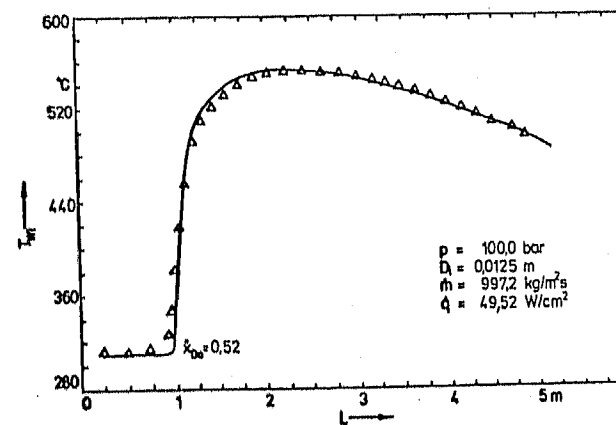

FIGURE 3. Post-dryout wall temperatures (Fluid water, measured data by KWU Δ, calculated by Schnittger ——)

The thermo- and fluiddynamic conditions become even more interesting if not a straight tube but a bend or coil is studied. Measurements in such geometrical configurations are presently performed by Lautenschlager /13/ and show that the bend produces a strong secondary flow of the vapour-droplet mixture.

Figure 4 presents the wall temperature and, by this, the heat transfer conditions circumferentially and longitudinally to the bended tube. The influence of the bend can even be realized some inches upstream before the bending starts.
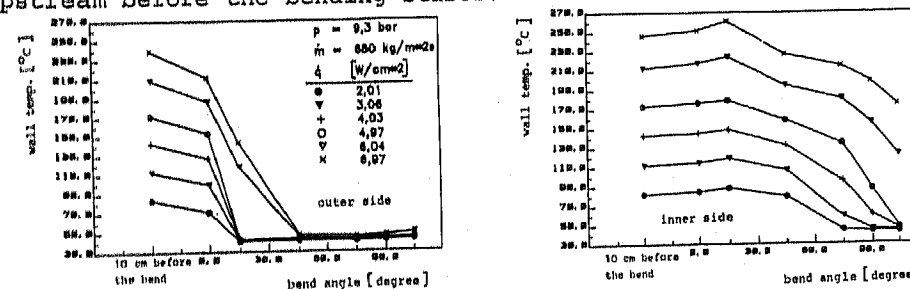

FIGURE 4. Heat transfer conditions along and around the wall of a bend.

From Fig.4 it can be seen that at first the heat transfer at the outer side of the bend improves, which easily can be explained by centrifugal forces enlarging the droplet concentration in this area. However, after a short distance also the heat transfer at the inner side of the bend is increasing which can be seen by the decreasing wall temperatures.

What is the reason for this unexpected phenomenon? Centrifugal forces produce a pressure drop over the cross section of the bended tube. This generates a secondary flow in such a way that in the center of the tube cross section there is an outward radial velocity due to centrifugal forces and at the tube wall, where friction prevails, there is an inward flow due to the mentioned pressure difference. This movement of the secondary flow improves the heat transfer conditions so that - compared to a straight tube - the overall heat transfer coefficient in a bended tube is always better. The secondary flow can even act to such an extent that the improved spray cooling allows a wetting of the wall also on the inner side of the bend. Post-dryout heat transfer or spray cooling, therefore, is not only a problem of thermodynamic nonequilibrium but also involves very complicated fluiddynamic processes. It would be worthwhile to study these processes and also the thermodynamic behaviour more in detail.

TRANSIENT CONDITIONS

Strong transient conditions occur with a pressure release which, for a water-cooled nuclear reactor, would be the case during a loss of coolant by accident. Pressure release in a vessel which is filled with liquid or vapour or both, which undergo the saturation condition, always causes a two-phase mixture. In the saturated liquid vapour bubbles are produced by flashing and, during the expansion of saturated vapour, liquid droplets are condensing. Both phase changes are combined with high energy transport between the phases and need a finite driving force to be started, which is well-known as boiling delay or condensation delay. Pressure release in fluids being originally in thermodynamic saturation condition, therefore, always causes at first and for a short period unstable conditions.

By measuring the time-depending pressure- and temperature-course during the depressurization - also called blowdown - we realize occurrences as demonstrated in Figure 5. The experimental results shown there were gained by Viecenz /14,15/ with a vessel of 0,5 m height and under the conditions of fast pressure release. The vessel was filled up to 1/3 with saturated liquid - refrigerant R12 - before the release started. The temporal course of the pressure release is expected to be influenced by foaming. By destroying a burst disk at the upper nozzle of the vessel the pressure in the vessel was released from approximately 10 bar to ambient pressure within about 15 s. After starting the pressure release it took a few tenths of a second until flashing started (A') and the pressure decrease during the period A is mainly due to the expansion of the vapour only in the vessel. The boiling delay more clearly can be seen from the temperature/pressure diagram in the lower part of Fig.5, which gives the information that during this period (A) the liquid temperature is remarkably higher than the saturation temperature, and also the vapour temperature is slightly above the saturation line. At point (A') flashing evaporation and, with this, bubble formation starts and during the period A'-C' the swell level is rising in the vessel. Due to its volumetric increase the flashing evaporation
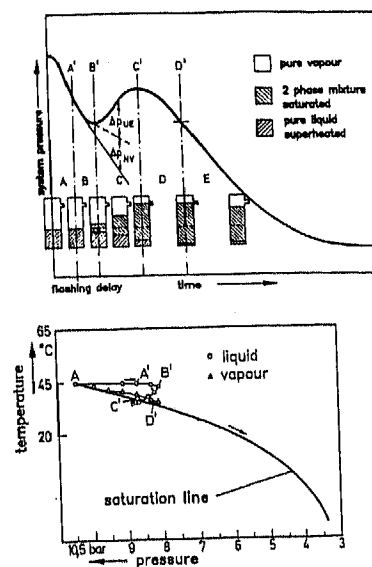

FIGURE 5. Pressure and temperature course during depressurization. Fluid: R12

during the period A'-C' is acting against the pressure decrease by loss of coolant out of the leakage. In the first part of the period B'-C' even more vapour is produced by flashing out of the superheated liquid than can flow out from the leakage. At the moment C' the swell level reaches the nozzle of the vessel. In the period B'-C' the superheating of the liquid is reduced strongly, as can be seen from the lower diagram in Fig.5. When the swell level reaches the nozzle (C') a two-phase mixture is now leaving the vessel and its mass flow rate is higher than that of pure vapour, which is the reason - together with the reduction in flash evaporation - that the pressure decreases again. This behaviour is mainly governed by the delayed vapour production on one side, and the phase separation on the other. For a better understanding and a more precise description of the blowdown we, therefore, need more information about phase separation.

Viecenz /14,15/ performed a detailed experimental and theoretical analysis of phase separation, based on the information available in the literature. He developed a correlation for the void fraction and also for the drift flux velocities of the phases. His void fraction correlation is presented in Figure 6.
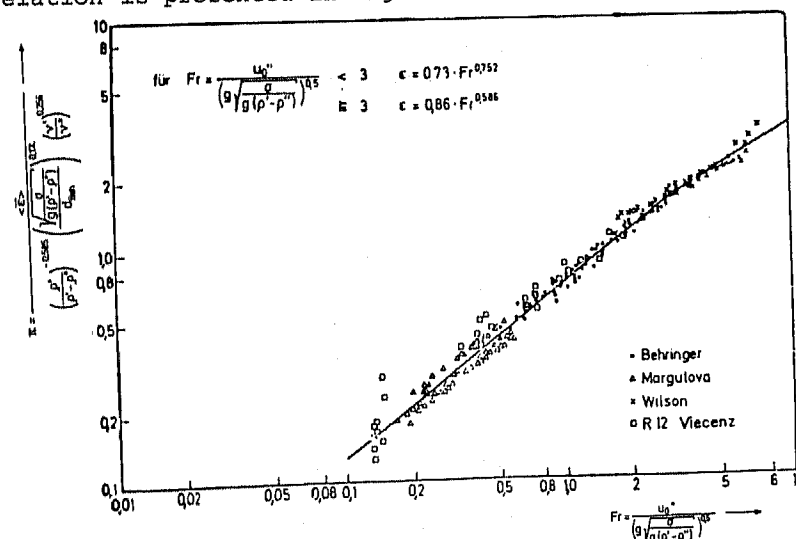

FIGURE 6. Void fraction as a function of Froude number.

The equation for the void fraction is mainly determined by a modified Froude-number in which the superficial velocity of the vapour, as characteristic velocity, is used. This superficial velocity is the velocity of the vapour, if it would flow in the empty vessel. In addition, the diameter of the bubbles is chosen as a characteristic length, and this bubble diameter is expressed by the Laplace-constant. At a Froude-number of 3 a change in the slope of the separation curve occurs. Therefore, the constant and the exponent with the Froude-number is changed at fluiddynamic conditions corresponding to a Froude-number 3. This discontinuous behaviour can be explained by the change in flow pattern at this Froude-number.

The correlation in Fig.6 at first was developed for steady-state flow conditions only. Using a computer program which predicts the time-depending evaporation rate in the liquid, this correlation, however, is also good for calculating the transient behaviour of the void fraction and the swell level during depressurization. A very careful and complicated energy balance, however, has to be used to get good results. Energy is stored in the superheated liquid and in the superheated vapour as long as thermodynamic equilibrium is not yet reached, and energy is also carried out of the vessel through the nozzle. This energy balance is linked with the continuity equation for mass and, therefore, in addition one needs a reliable correlation for critical mass flow rate. The detailed correlation procedure is explained in /14/.

Results gained with these correlation methods are presented in Figure 7, for an example with a large leakage opening, i.e. a fast and violent blowdown where the foaming mixture reaches the nozzle within about half a second. For comparison sake also other phase separation models - as for example presented by Wilson /16/ or Zuber /17/ - were used in the mentioned calculation procedure and the results are shown in Fig.7, too.
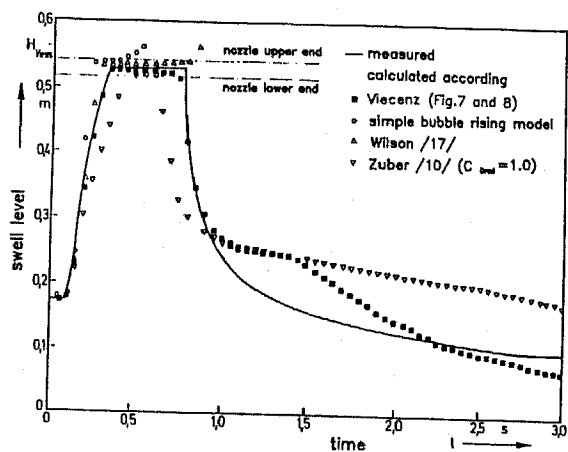

FIGURE 7. Comparison of measured and calculated swell level during a blowdown in a vessel.

Another type of transient conditions occur in a nuclear reactor, if the primary fluid circulating pumps fail due to a station blackout, or if a control rod would be suddenly withdrawn. Boiling crisis could occur in such a situation on the fuel rods, which could endanger the cladding.

The inertia of the rotating parts of the pumps and also of the liquid mass in the loop is so large that it would take seconds or even minutes until the mass flow rate is substantially reduced. Hein /18/ and Moxon /19/ measured the critical heat flux under the transient conditions of reducing the driving heat of the pump. They found that with a failure of the pumps the critical heat flux can be predicted fairly well by assuming quasi-steady conditions. Quasi-steady state has to be interpreted here in such a way that the calculation always assumes thermodynamic equilibrium by using one of the burn-out equations well-known from the literature /20/. Results calculated by this method and measured data are compared in Figure 8.
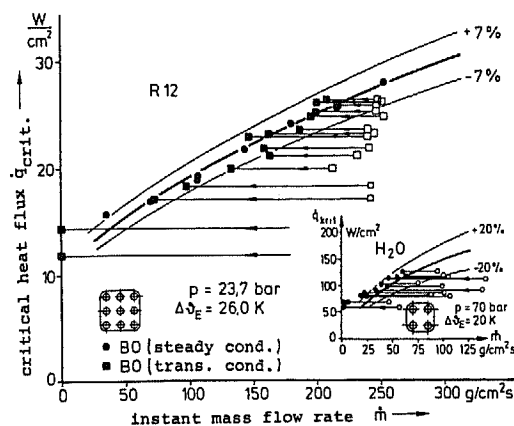

FIGURE 8. Critical heat flux with loss of flow.

This figure has to be interpreted in the following way:
Starting from a steady-state condition (empty symbols) the mass flow rate was lowered along the horizontal lines, marked in the figure with arrows, that is under constant heat flux conditions. This mass flow reduction was continued until boiling crisis occurred, which is marked with the full symbols. For comparison, critical heat flux as it would occur under steady-state conditions is given in the figure as full-line curve, which is calculated from an equation of the literature. The figure gives results for water and for the refrigerant R12. One can see that the transient data fall well together with the steady-state predictions. Only at very low mass flow rates there are deviations. Here, however, one has to realize that buoyancy forces influence the flow behaviour.

One can also imagine incidents in which the heat addition to a boiling channel is suddenly increased and then the question raises, which criteria are valid for predicting the onset of the boiling crisis. Hein and Kastner /21/ found that very rapid power excursions allow much higher heat flux densities until boiling crisis occurs than it is the case under steady-state conditions. Figure 9 shows that with these power excursions critical heat flux densities can be reached, which are by a factor of 1,5 - 3 higher than those in steady-state situation.

Arguing why steep power excursions allow such high heat fluxes, one has to take in account different phenomena, well known from fluiddynamics and heat transfer. At first it needs a certain time until nucleate boiling changes in film boiling, that is until the dry patch at the wall can be formed by evaporating the liquid film there.
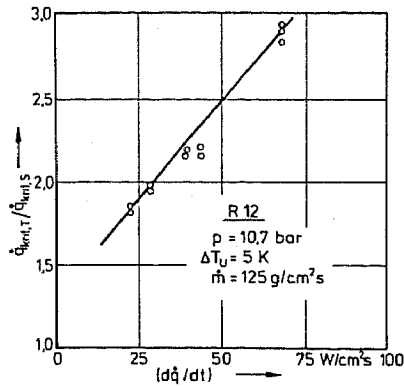
FIGURE 9. Critical heat flux with sudden power excursions (index T = transient conditions; S = steady-state conditions.)

By this, automatically a progression of the critical heat flux density is given with decreasing time period of the power transient. By evaporating liquid upstream of the position where the boiling crisis in the channel will occur, a violent acceleration of the flow is generated during this short power excursion, which improves the heat transfer remarkably. The liquid layer at the wall shows, with accelerated flow, a steeper temperature profile than with steady-state conditions.

SCALING

Transducing results from experimental models to original conditions of large power plants or chemical installations is an old engineering problem. The scaled-down model has to be similar to the original with respect to its geometrical design, its fluiddynamic phenomena and its thermodynamic conditions. In two-phase flow scaling is usually not practiced via reducing the dimensions but by using another substance, a so-called modelling fluid, with lower latent heat of evaporization. So scaling the thermodynamic properties becomes an important problem. Scaling criteria for two-phase flow, especially also with respect to thermodynamic similarity, are discussed in detail in /22-24/.

In the literature thermodynamic properties usually are scaled by using the same density ratio between liquid and vapour for the modelling experience as under original conditions. If there would exist a universal equation of state for all substances, one could show that scaling of the properties could be successfully performed via the thermodynamic consistency using the theorem of corresponding states. In /22,24/ is shown that already the Van der Waals-equation can serve for a first step in this direction by reducing the data with the critical values. By applying the data to the reduced pressure, not only transport properties like viscosity and thermal conductivity but also caloric properties and even their derivatives show similar behaviour for different fluids over a wide range of thermodynamic conditions. In Figure 10 examples of viscosity and the derivative of the latent heat of evaporization with respect to pressure are shown for the substances water and refrigerant R12. By applying a constant multiplier for the relevant property almost full agreement can be reached in the course of the curves over the
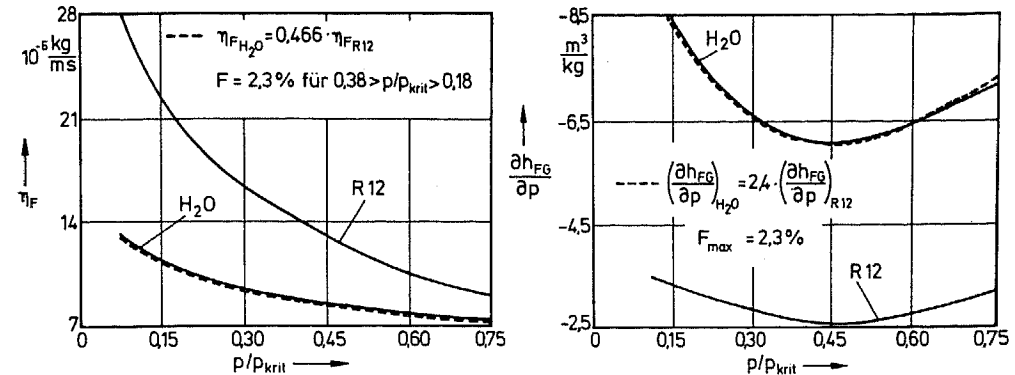

FIGURE 10. Scaling of thermodynamic properties, a) viscosity of liquid, b) derivative of latent heat of evaporization with respect to pressure.

pressure along the saturation line, as shown in Fig.10. This means that the thermodynamic condition can be advantageously scaled by using the same reduced pressure in the modelling experiment as in the original. The multiplier then resulting from the properties adjustment has to be taken in account with defining the fluiddynamic parameter, for example the Reynolds-number, by choosing a velocity in the modelling experiments which balances the multiplier in the viscosity. Scaling complicated situations in two-phase flow apparatus is difficult, however possible by this method, as demonstrated in /20,22,23/. Even the fluiddynamic and thermodynamic conditions during the blowdown of a nuclear reactor can be scaled by this method with the modelling fluid R12, as Figure 11 shows.
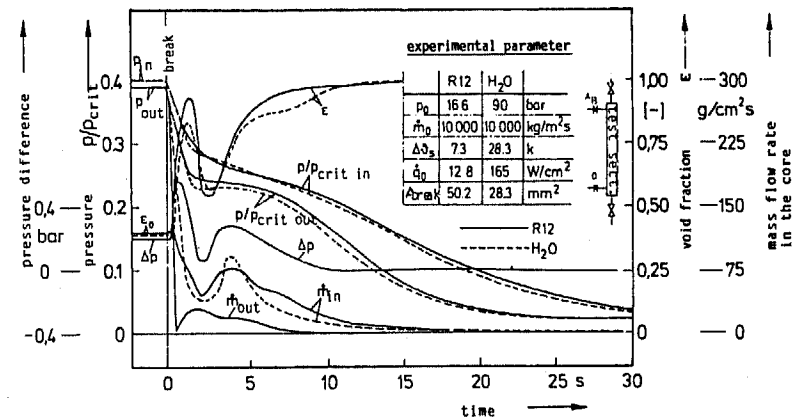

FIGURE 11. Experimental data during a blowdown (loss of coolant accident); comparison of tests performed in a water facility and in a R12-loop.

Two different experiments performed at two different institutions - one using water, the other one R12 - are compared there. The geometrical dimensions in both experiments were extendingly identical.

The comparison encourages to draw the conclusion that also in transient two-phase flow scaling is possible, even if the interesting phenomena are complex and fluiddynamically coupled.

LITERATURE

1. Hutchinson,P.; Whalley,P.B. Chem.Eng.Sci.28 (1973),26.

2. Keeys,R.K.; Ralph,R. AERE-Report No.6294 (1970).

3. Wicks,M.; Dukler,A.E. AICHE Journal 6(1960) 463.

4. Collier,J.G.; Hewitt,G.F. Trans.Inst.Chem.Eng.39 (1961),127.

5. Langner,H.; Diss., Techn.Univ.Hannover, 1978.

6. Nordmann,D.; Diss., Univ.Hannover, 1980.

7. Chen,Y.M.; Diss.Techn.Univ.München, 1985.

8. Iloeje,O.C.; Plummer,D.N.; Rohsenow,W.M.; Griffith,P.; MIT Dept.of Mech.Engng., Report 72718-92, Sept.1974.

9. Plummer,D.N.; Ph.D.Thesis,Massachusetts Inst.of Techn.,May 1974.

10. Ganic,E.N.; Rohsenow,W.M. Int.J.Heat/Mass Transf.20,855 (1977).

11. Groeneveld,D.C.; Delorme,G.G.I.; Nuclear Engineering and Design 36, 17-26, North Holland Publishing Company, 1976.

12. Schnittger,R.B.; Diss.Univ.Hannover, 1982.

13. Lautenschlager,G.; Unpublished information.

14. Viecenz,H.J.; Diss.,Univ.Hannover, 1980.

15. Viecenz,H.J.; Mayinger,F.; Two-Phase Flows and Heat Transfer, Hemisphere Publ.Corporation, New York, 1348-1404, 1978.

16. Wilson,J.F. et al. Trans.Am.Nuc.Soc.4 No.2, 1961.

17. Zuber,N.; Findley,J.A.; Transaction of the ASME, Journal of Heat and Mass Transfer, Vol.87 (1965), 453-468.

18. Hein,D.; Kastner,W.; M.A.N.- Report No.45.03.02.

19. Moxon,D.; Edwards,P.A.; European Two-phase Heat Transfer Meeting, Bournemouth, and AEEW-R 553, 1967.

20. Mayinger,F.; Strömung und Wärmeübergang in Gas/Flüssigkeits-Gemischen, Springer-Verlag, Wien - New York, 1982.

21. Mayinger,F., et al. Brennst.-Wärme-Kraft 18(1966)No.6,288-294.

22. Ishii,M.; Jones,O.C.jr.; Derivation and application of scaling criteria for two-phase flows, Hemisphere Publ.Corp.,163-185,1976.

23. Mayinger,F.; Scaling and modelling laws in two-phase flow and boiling heat transfer, Proceedings of NATO Advanced Study Inst., "Two-Phase-Flows and Heat Transfer", Hemisphere Publ.Corp., Vol.1, 129-161, Washington, 1976.

Dropwise Condensation—Progress toward Practical Applications

ICHIRO TANASAWA
Institute of Industrial Science
University of Tokyo
Tokyo, Japan

1. INTRODUCTION

At the Sixth International Heat Transfer Conference held at Toronto, Canada in 1978, the author was given an opportunity to deliver a keynote lecture entitled "Dropwise Condensation — The Way to Practical Applications[89]." In this lecture the author presented a state-of-the-art review on the study on dropwise condensation and showed the author's personal outlook upon the future investigation aiming at practical applications. In addition to this, the author published a monograph[77] and a couple of reviews[75,92] on dropwise condensation almost at the same time. The monograph[77], which is of about one hundred pages, has very detailed contents, the results of early researches and the studies on the microscopic mechanisms of dropwise condensation being extensively introduced.

Since then, a considerable progress has been made in the research on dropwise condensation. A main objective of this paper is to supplement the four articles cited above, reviewing the results of studies on dropwise condensation carried out during the last decade since 1975 and reconsidering about the problems to be solved before the practical application of dropwise condensation results in success. However, some of the results of researches published prior to 1975 are also quoted for the convenience of readers.

2. MEASUREMENT OF HEAT TRANSFER COEFFICIENT

The experimental studies on the heat transfer by dropwise condensation have been carried out only under very limited conditions. It is only recently that the data on the heat transfer coefficient of dropwise condensation of steam at atmospheric pressure have been put in order. Those data for other vapors and the measurements under different thermal conditions are still scarce. Therefore, the description which follows is mostly concentrated on dropwise condensation of steam at atmospheric pressure.

2.1 Results of measurements on steam at 1 atm

Since the first observation by Schmidt et al.[2] the heat transfer coefficient of dropwise condensation of steam near 1 atm has been measured by a lot of researchers. The results have been summarized by Tanner et al.[26], Graham[45], and Tanasawa[77,89,92], showing a considerably wide scattering. However, since the experimental techniques have made a great progress during these fifteen years, the reproducibility and reliability of the experimental data have been established to some extent. We owe much to several investigators such as Le Fevre and Rose[21,25], and Citakoglu and Rose[40]. At present, we can say that the heat